Front. Electr. Electron. Eng. China 2008, 3(4): 480–487
DOI 10.1007/s11460-008-0072-9

RESEARCH ARTICLE

Jufan ZHANG, Bo WANG, Shen DONG

Application of atmospheric pressure plasma polishing method in machining of silicon ultra-smooth surfaces

Abstract The modern optics industry demands rigorous surface quality with minimum defects, which presents challenges to optics machining technologies. There are always certain defects on the final surfaces of the components formed in conventional contacting machining processes, such as micro-cracks, lattice disturbances, etc. It is especially serious for hard-brittle functional materials, such as crystals, glass and ceramics because of their special characteristics. To solve these problems, the atmospheric pressure plasma polishing (APPP) method is developed. It utilizes chemical reactions between reactive plasma and surface atoms to perform atom-scale material removal. Since the machining process is chemical in nature, APPP avoids the surface/subsurface defects mentioned above. As the key component, a capacitance coupled radio-frequency plasma torch is first introduced. In initial operations, silicon wafers were machined as samples. Before applying operations, both the temperature distribution on the work-piece surface and the spatial gas diffusion in the machining process were studied qualitatively by finite element analysis. Then the following temperature measurement experiments demonstrate the formation of the temperature gradient on the wafer surface predicted by the theoretical analysis and indicated a peak temperature about 90°C in the center. By using commercialized form talysurf, the machined surface was detected and the result shows regular removal profile that corresponds well to the flow field model. Moreover, the removal profile also indicates a 32 mm^3/min removal rate. By using atomic force microscopy (AFM), the surface roughness was also measured and the result demonstrates an Ra 0.6 nm surface roughness. Then the element composition of the machined surface was detected and analyzed by X-ray photoelectron spectroscopy (XPS) technology. The results also demonstrate the occurrence of the anticipated main reactions. All the experiments have proved that this atmospheric pressure plasma polishing method has the potential to achieve the manufacture of high quality optical surfaces.

Keywords atmospheric pressure plasma, ultra-smooth surface, single crystal silicon, capacitance coupled, polishing

1 Introduction

The modern optics industry demands rigorous surface quality, which presents challenges to optics machining technology. Some optical components emphasize quite a low surface roughness or scattering characteristics to obtain maximum reflectivity. For functional demand, the integrity of surface lattice is always top-priority as most applicable materials are brittle. Both the surfaces mentioned above can be defined as “ultra-smooth surface” which takes the surface roughness less than 1 nm and minimal surface/subsurface defects as main features [1].

In practical manufacturing systems, conventional mechanical technologies, such as slicing, lapping and polishing, play an important role. Although satisfying surface roughness can be obtained, the removal rate is usually too low for many applications. For example, the surface roughness of the laser gyroscope mirror is required to reach about 2 Å R_q, which will take seven days at least to achieve with conventional polishing technologies. It does slow down the equipping pace of weapon types. It is especially serious for hard brittle functional materials, such as crystal, glass and ceramics, due to their special characteristics. Furthermore, when polishing a component with the SiC layer on the outmost surface, because of high hardness, the machining stress is even more than four times larger than that of polishing glass and ceramic, which may cause destructive damage when it meets very thin light weight mirrors. Moreover, the contacting mechanical technologies always introduce various defects on

Translated from *Optics and Precision Engineering*, 2007, 15(11): 1749–1755 [译自: 光学精密工程]

Jufan ZHANG (✉), Bo WANG, Shen DONG
School of Mechanical Engineering, Harbin Institute of Technology, Harbin 150001, China
E-mail: zhangjufan@hotmail.com

the final surfaces of optical components, such as plastic deformation, brittle fracture, dislocation, micro-cracking, etc. These defects present in crystalline or amorphous substrates will lower the damage threshold for high fluence use or increase the chemical activity of the surface for corrosion. Therefore, the conventional contacting machining technologies are not suitable for functional materials with excellent physical properties that demand a perfect crystal structure. Thus, the manufacturing of ultra-smooth surfaces with minimum surface/subsurface defects strongly demands the development of new machining methods with no surface contact.

To solve the problems mentioned above, much effort has been devoted to the research on the formation mechanism of ultra-smooth surface and relevant surface detection technologies, making many non-contacting precision machining methods come into applications. These innovative methods have brought in completely new machining mechanisms and devices. They perform the atom/molecule scale material removal by chemical or physical actions and represent the development trend of the manufacturing technology used for high quality optical surfaces. As a representative branch, the plasma assisted surface processing technology has been used in a wide range of applications for a long time due to its unique advantages, such as low cost, no waste, no contamination, and especially the excellent surface quality which is difficult to obtain by conventional machining technologies. There are already many typical technologies based on plasma process, such as reactive ion etching (RIE), plasma assisted chemical etching (PACE), ion beam milling, etc [2,3]. However, these earlier technologies all need vacuum systems to support, with rigorous requirements of the whole equipment. Thus, some researchers have proposed to develop a plasma machining process in atmospheric environment. Atmospheric pressure plasma technology can generate uniform low temperature plasma in a large area. It has a lower cost on equipment and maintenance as well as more extensive application range. Low temperature plasma contains more multifarious and energetic active species than those generated from chemical reactions, which makes it easier to react with materials. Majority of low temperature plasma are neutral particles and ions, both of which are at environmental temperature. Also, the minor high energy electrons provide the activation energy for the chemical reactions. Generally, the density of atmospheric pressure plasma is four orders of magnitude higher than that of vacuum plasma. The active radical's density is at least two orders of magnitude higher than that of plasma to maintain a high efficiency.

Nowadays, several institutes have done some research to develop the atmospheric pressure plasma machining technology. The Lawrence Livermore National Laboratory in the US has developed the reactive atom plasma technology (RAPT) which adopts the inductively coupled plasma (ICP) torch as the source [4]. The Osaka University in Japan has developed the plasma chemical vaporization machining (PCVM) method. PCVM utilizes various types of rotary electrodes to generate reactive plasma [5,6]. Researchers at Harbin Institute of Technology in China have developed the atmospheric pressure plasma polishing (APPP) method [7,8]. The APPP method introduces the capacitance coupled radio frequency plasma torch as the source [9]. It utilizes the atmospheric pressure plasma to excite reactive radicals, which then cause chemical reactions with the surface atoms to perform atom scale material removal. Since the machining process is chemical in nature, APPP avoids various surface/subsurface defects which usually appear in mechanical machining process.

2 Principle and system

In normal machining process, the reaction gas and plasma gas with optimum ratio is sufficiently mixed and then input into the plasma torch. Then, ionized by the radio-frequency (RF) power, the reaction gas is excited in the plasma to generate high density and high energy reactive radicals. Then the generated reactive radicals cause chemical reactions with the surface atoms of the work-piece, which performs the effective atom-scale material removal, as shown in Fig. 1.

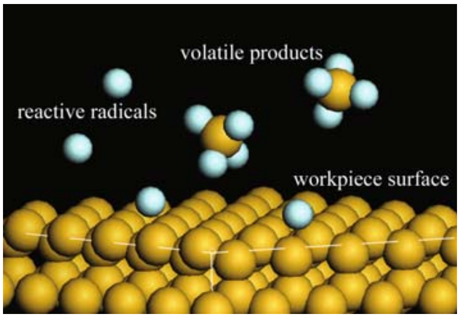

Fig. 1 Principle of APPP method

For different materials, appropriate recipes should be considered. For example, in initial operations silicon, wafers are selected as samples, thus He gas can be adopted as plasma gas while CF_4 gas works as the reactive precursor. He gas is excited to form a stable non-thermal equilibrium plasma. Then, excited by plasma, some CF_4 is converted to radical F^* atoms which are chemically active. Radical F^* atoms cause chemical reactions with surface Si atoms generating SiF_4 product. Because the product is the volatile gas that tends to vent, the machined surface left behind introduces no contaminant. Since it has been proved that the plasma is chemical in nature, the APPP method is capable of avoiding surface/subsurface damage.

A capacitance coupled radio-frequency plasma torch has been developed for the APPP method. High density reactive radicals can be generated at atmospheric pressure using this self-fabricated torch. The plasma source arranges two water-cooled electrodes as a coaxial torch structure based on capacitance coupled principle. The outer cathode connects to the ground while the inner anode connects to the RF power. There is a separating structure made by highly insulative material in the fixation portion, as shown in Fig. 2. The shape of the plasma flame produced by this torch is easy to regulate.

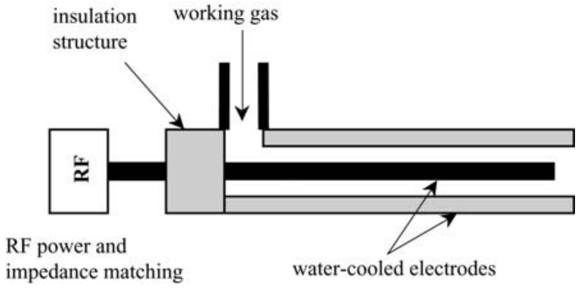

Fig. 2 Schematic diagram of capacitance coupled radio-frequency plasma torch

The plasma torch is where the plasma and reactive radicals are generated. Many factors that will affect the discharge state and plasma characteristics should be considered in the design and fabrication process. First, since aluminum is selected as the electrode material, the Al_2O_3 layer should be formed on the outmost surface of the anode by micro-arc oxidation technique to avoid drawn arc between electrodes. Second, a slight burr on the electrode's surface will cause a fluctuation in plasma or even terminate the discharge, thus, a precision machining process should be performed when manufacturing electrodes. Third, the environment with useless gases will influence the discharge status. Therefore, keeping the gas path hermetic is important. Finally, the ratio and speed of the mixed gas notably affects the density and energy of reactive radicals, and even a slight change will result in an obvious fluctuation. Hence, a mass flow controller is necessary. As the key component of the APPP system, the capacitance coupled radio-frequency plasma torch also needs peripherals to support, such as a gas supply system, RF power supply and impedance matching system, multi-axes worktable and relevant motion control system, hermetic chamber, and residual gas recovery system, etc.

3 Demonstration of system validity

Experiments were conducted to verify the function of the designed plasma torch. All the experiments mentioned below were performed under atmospheric pressure and room temperature. By using the atomic emission spectroscopy analysis, categories and relative densities of major atoms in the plasma zone can be obtained. A commercialized micro-fiber-spectrometer is used to detect the atomic emission spectrometry. First, the plasma was initially generated by exciting helium gas only. Adjusting the RF power to 200 W, there appeared a visible flame near the outlet, which indicated the plasma. The discharge was stable and the phenomenon was obvious. With the RF power rising, the flame became brighter while the density of the ionized atoms also increased. Under a 600 W RF power and 40 SLM (standard L/min) helium gas flow only, high density low temperature plasma was formed, as shown in Fig. 3. Then, a trace of CF_4 gas was introduced into the plasma torch, making the atom composition of the plasma zone change remarkably. Reactive radical F^* atoms appeared, as Fig. 4 shows. According to Fig. 4, there are ten new spectral lines appearing obviously in the spectrogram, which indicates fluorine atoms at different excited states, including three most intelligent lines [10]. It offers a powerful evidence for the validity of the designed plasma torch.

Furthermore, each spectral line in Fig. 4 indicates a certain atom state. In normal conditions, the atom is on the ground state. If it is excited and obtains enough energy, the outer-shell electron will transit to an excited state with higher energy level. Because the electron on the excited state is unstable and has a life time of less than 10^{-8} s, it will jump back to a lower energy state or the ground state. As a result, the excess energy emits as electromagnetic radiation, forming the atomic emission spectrum. The spectrum wavelength and corresponding energy follow the next equation [11]:

$$\lambda = \frac{hc}{E_2 - E_1}, \tag{1}$$

where E_1 is the energy of the lower level while E_2 is the energy of the higher level; λ is the wavelength; h is the Planck constant; c is the velocity of light. Thus, for the spectrogram shown in Fig. 4, for example, there is a spectral line which corresponds to the 685.60 nm wavelength. It can be calculated from Eq. (1) that the energy difference between the two levels is 1.8079 eV. The National Institute of Standards and Technology (NIST)/ Atomic Spectra Database/Levels Data (http://physics.nist.gov/PhysRefData/ASD/index.html, 2007) indicates that the transition is from the $2s^22p^4(^3P)3p\ ^4D^\circ\ ^7/_2$ orbit to the $2s^22p^4(^3P)3s\ ^4P\ ^5/_2$ orbit. Likewise, other spectral lines' can also be found in the same way, as shown in Table 1. The data are necessary for further researches on microcosmic mechanism analysis.

4 Experiments and discussion

Because of the annular outlet of the plasma torch, the plasma flame will change its shape if the gas diffusion alters. This problem was first studied by finite element analysis method in theory and then demonstrated by

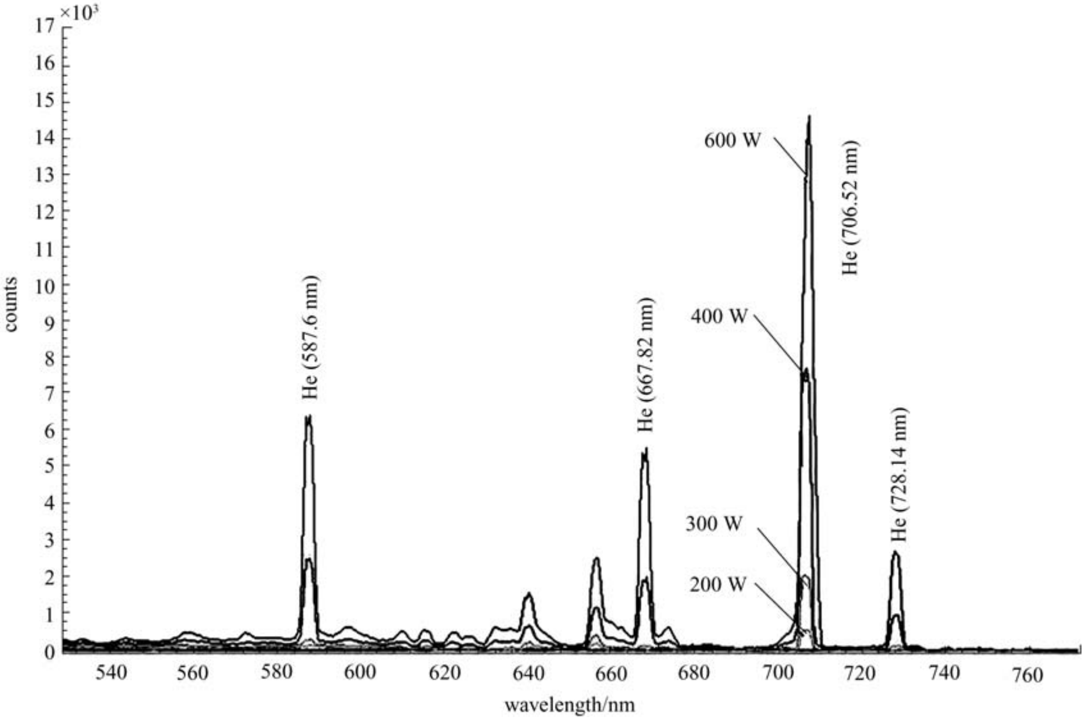

Fig. 3 Helium plasma spectrogram (200 W, 300 W, 400 W, 600 W, He 40 SLM)

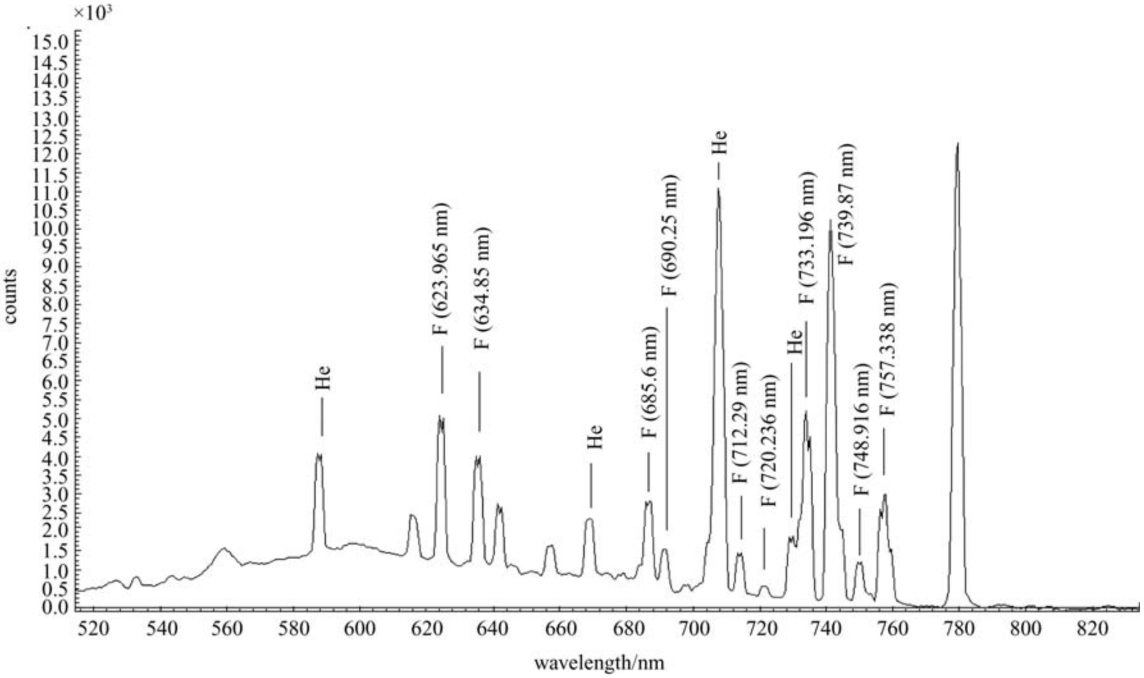

Fig. 4 Reactive plasma spectrogram (RF power 600 W, He 40 SLM, CF_4 0.35 SLM)

experiments. Figure 5 shows the theoretical gas diffusion model made by commercialized software (Fluent 6.1; Fluent Inc., Lebanon, NH, USA) based on finite element analysis principle. The state inside the plasma torch is irrelevant to this process. What is more important is the condition where the gas and reactive atoms flow out from the torch and further diffuse outwards. In consideration of the rotational symmetrical characteristics of the gas path, a two-dimensional cross-sectional view is used to explain this problem. The results can be extended to three-dimensional space because the cross-sectional view is intercepted from the spatial model. The gray blocks in Fig. 5 indicate the work-piece and torch entity, and the paths *A* and *B* indicate the gas diffusion paths. After flow-

Table 1 Wavelength and corresponding transition of radical fluorine atoms in spectrogram

wavelength/nm	transition between orbits
623.965	$2s^22p^4(^3P)3s\ ^4P\ ^5/_2 - 2s^22p^4(^3P)3p\ ^4S^\circ\ ^3/_2$
634.851	$2s^22p^4(^3P)3s\ ^4P\ ^3/_2 - 2s^22p^4(^3P)3p\ ^4S^\circ\ ^3/_2$
685.603	$2s^22p^4(^3P)3s\ ^4P\ ^5/_2 - 2s^22p^4(^3P)3p\ ^4D^\circ\ ^7/_2$
690.247	$2s^22p^4(^3P)3s\ ^4P\ ^3/_2 - 2s^22p^4(^3P)3p\ ^4D^\circ\ ^5/_2$
712.789	$2s^22p^4(^3P)3s\ ^2P\ ^1/_2 - 2s^22p^4(^3P)3p\ ^2P^\circ\ ^1/_2$
720.236	$2s^22p^4(^3P)3s\ ^2P\ ^1/_2 - 2s^22p^4(^3P)3p\ ^2P^\circ\ ^3/_2$
733.196	$2s^22p^4(^3P)3s\ ^4P\ ^5/_2 - 2s^22p^4(^3P)3p\ ^4P^\circ\ ^3/_2$
739.87	$2s^22p^4(^3P)3s\ ^4P\ ^3/_2 - 2s^22p^4(^3P)3p\ ^4P^\circ\ ^1/_2$
748.916	$2s^22p^4(^3P)3s\ ^2P\ ^1/_2 - 2s^22p^4(^3P)3p\ ^2S^\circ\ ^1/_2$
757.338	$2s^22p^4(^3P)3s\ ^4P\ ^1/_2 - 2s^22p^4(^3P)3p\ ^4P^\circ\ ^3/_2$

ing out from the plasma torch, some gas containing reactive radicals will finally diffuse outwards to the air, while the other part carrying reactive radicals will diffuse into the central area. The central area *C* is a turbulence region because both the gas paths *A* and *B* supply gas to this area in opposite directions. Just due to this dual supply, the density of the radical atoms is maintained at approximately double amount from the two paths respectively, while the outside areas are only supplied by one path. Thus, the removal rate in the center should be the highest, and decrease gradually toward the outside. This means that the practical removal shape should be a single large pit with the depth decreasing away from the center.

The subsequent experiment has proved the theoretical analysis above. Figure 6 shows the actual removal profile in the practical operation. It is clear that the removal profile is of 40 μm depth in the center after ten minutes machining. Therefore, the peak removal rate in depth is about 4 μm/min. In consideration of the rotational symmetrical characteristics of the removal shape, the removal rate in volume can be calculated from the contour in the cross-sectional view. By calculation, it is demonstrated that the removal rate reaches about 32 mm^3/min on single crystal silicon.

In the first section, it has been mentioned that the Lawrence Livermore National Laboratory in the U.S. has developed the RAPT. Researchers in Cranfield University in the U.K. have utilized this technology to machine ultra-low expansion (ULE) glass and indicate that the maximum sample temperature can reach about 220°C [12]. Correspondingly, the APPP method uses low temperature plasma to avoid local high temperature on the part surface. By finite element analysis, the heat distribution on the work-piece surface is first studied. The qualitative result indicates that obvious temperature gradient should be formed in the process, as shown in Fig. 7.

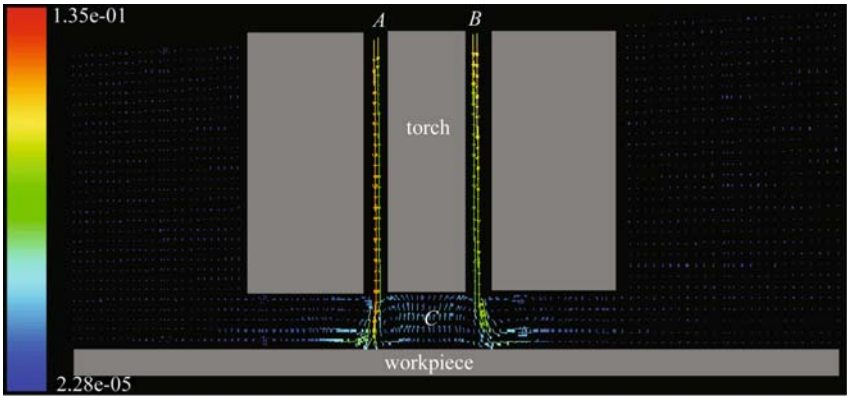

Fig. 5 Theoretical model of spatial flow field distribution

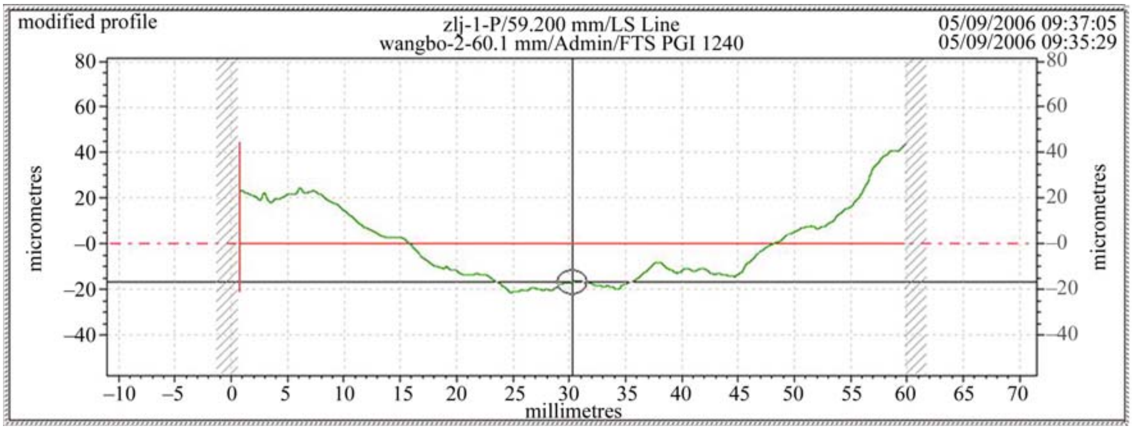

Fig. 6 Image of practical removal profile detected by form talysurf

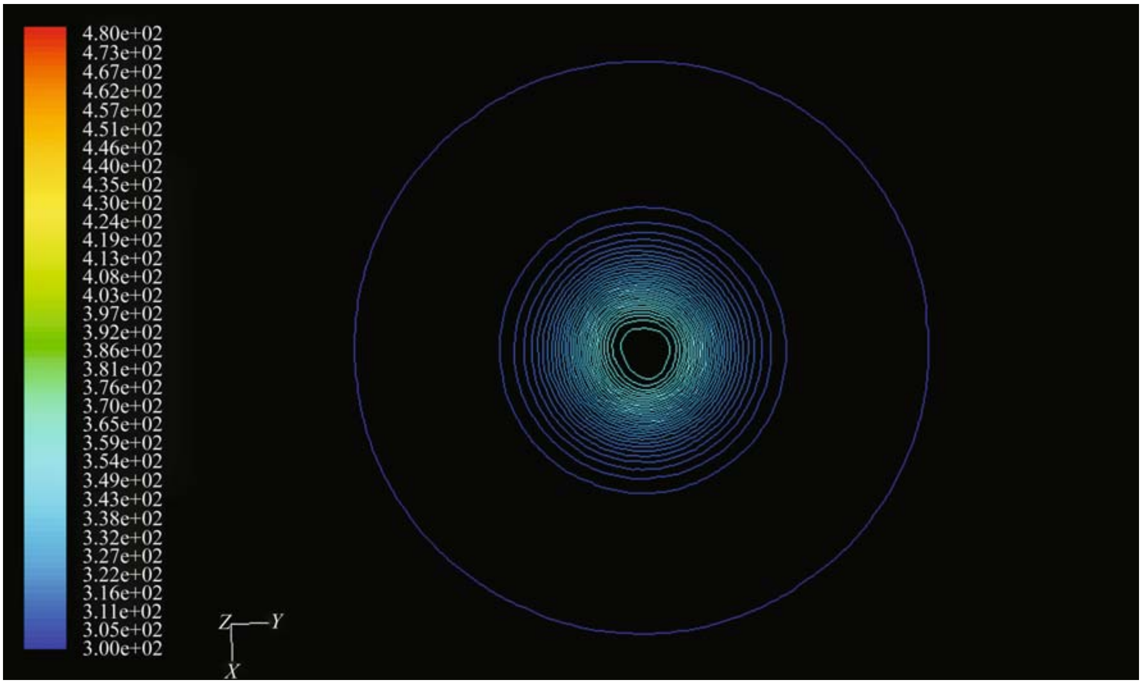

Fig. 7 Theoretical model of temperature distribution on work-piece surface

By real-time measuring on specified spots, as Fig. 8 shows, the temperatures on the part surface at different moments can be recorded. After a period of rise and feeble fluctuation, all the temperatures stayed stable as shown in Table 2. The values in this table are approximate in consideration of the impact introduced by the environment and devices. The test result indicates certain temperature gradient on the wafer surface, which agrees well with the theoretical simulation qualitatively.

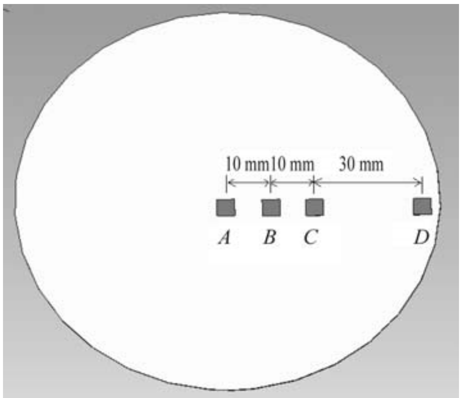

Fig. 8 Locations of measuring spots in temperature monitoring experiment

Table 2 Final temperatures of different measuring spots in Fig. 8

spot	temperature/°C
A	90
B	80
C	76
D	67

5 Surface characteristics detection

Before and after machining, the surface roughness in the same region was detected by atomic force microscopy (AFM, Dimension 3100, Digital Instruments Inc., USA). It is clear by contrast that the APPP method has achieved very good surface quality. Figure 9 shows the accurate values of the surface roughness. It indicates that the surface roughness is lower by more than 1 nm after machining and reaches about Ra 0.631 nm. Therefore, it can be said that this APPP method has the potential to support the sub-nanometer scale machining process to obtain high quality ultra-smooth surfaces.

After machining, the element composition of the machined region was also detected by X-ray photoelectron spectroscopy (XPS, PHI 5700 ESCA system, Physical Electronics, Chanhassen, MN, USA). Figure 10(a) shows the general analysis result. It is clear that there are four elements, Si, F, O and C appearing on the machined surface, where most of the O and C element was from the air and deposited on the surface when the surface was exposed to the environment. Some parts were maybe from the recipe gas when the chemical reaction progressed, which needs proving by further research. These two elements are by-products of this process that should be eliminated. Si and F are the main elements participating in this reaction with multiple ways to combine. In theory, some F atoms will bond with the Si atoms on the outer layers and perform the chemical adsorption on the surface [13,14]. Thus, the existing F element offers the evidence for the occurrence

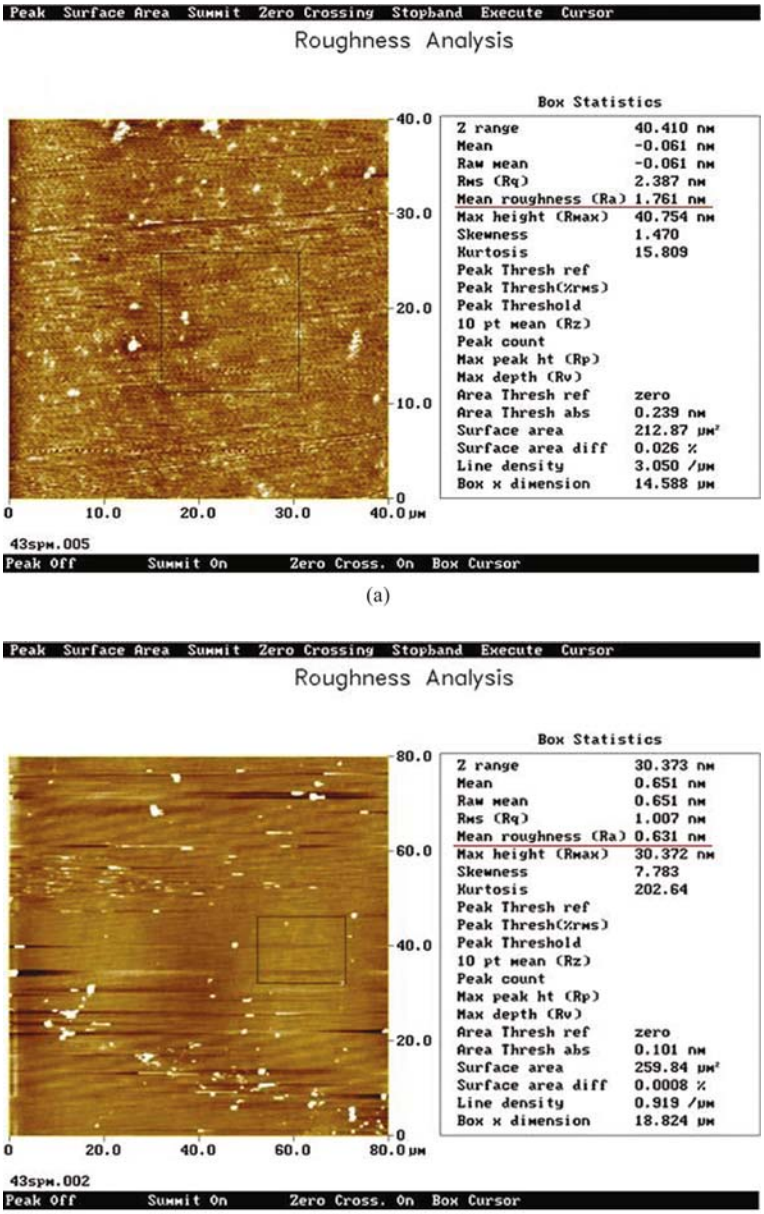

```
Box Statistics
Z range                40.410 nm
Mean                   -0.061 nm
Raw mean               -0.061 nm
Rms (Rq)               2.387 nm
Mean roughness (Ra)    1.761 nm
Max height (Rmax)      40.754 nm
Skewness               1.470
Kurtosis               15.809
Peak Thresh ref
Peak Thresh(%rms)
Peak Threshold
10 pt mean (Rz)
Peak count
Max peak ht (Rp)
Max depth (Rv)
Area Thresh ref        zero
Area Thresh abs        0.239 nm
Surface area           212.87 µm²
Surface area diff      0.026 %
Line density           3.050 /µm
Box x dimension        14.588 µm
```

(a)

```
Box Statistics
Z range                30.373 nm
Mean                   0.651 nm
Raw mean               0.651 nm
Rms (Rq)               1.007 nm
Mean roughness (Ra)    0.631 nm
Max height (Rmax)      30.372 nm
Skewness               7.783
Kurtosis               202.64
Peak Thresh ref
Peak Thresh(%rms)
Peak Threshold
10 pt mean (Rz)
Peak count
Max peak ht (Rp)
Max depth (Rv)
Area Thresh ref        zero
Area Thresh abs        0.101 nm
Surface area           259.84 µm²
Surface area diff      0.0008 %
Line density           0.919 /µm
Box x dimension        18.824 µm
```

(b)

Fig. 9 Images of surface roughness detected by AFM. (a) Before machining: Ra 1.761 nm; (b) after machining: Ra 0.631 nm

of the anticipated main reactions. However, the Si element performs actively in this process and produces various products. Besides reacting with F atoms to generate SiF_4 gas product, Si atoms also bond with O atoms to produce SiO_2 on the surface, as shown in Fig. 10(b). The left peak with lower binding energy indicates single crystal silicon and the right peak with higher binding energy indicates silicon oxide. By comparison, it is clear that the amount of the single crystal silicon is much larger than that of silicon oxide. Thus, by further theoretical analysis on the chemical process on the gas-solid interface, there should be some way to restrain the side reactions [15].

6 Conclusions

To produce high quality optical surfaces, the atmospheric pressure plasma polishing method is developed. It utilizes low temperature plasma chemical process to perform atom-scale material removal and avoid the surface/subsurface defects. A capacitance coupled radio frequency plasma torch is first introduced to manufacture the ultra-smooth surfaces. Experiments were conducted to demonstrate the validity of the self-fabricated system. An effort to achieve a tune of the whole system also makes the entire equipment work well.

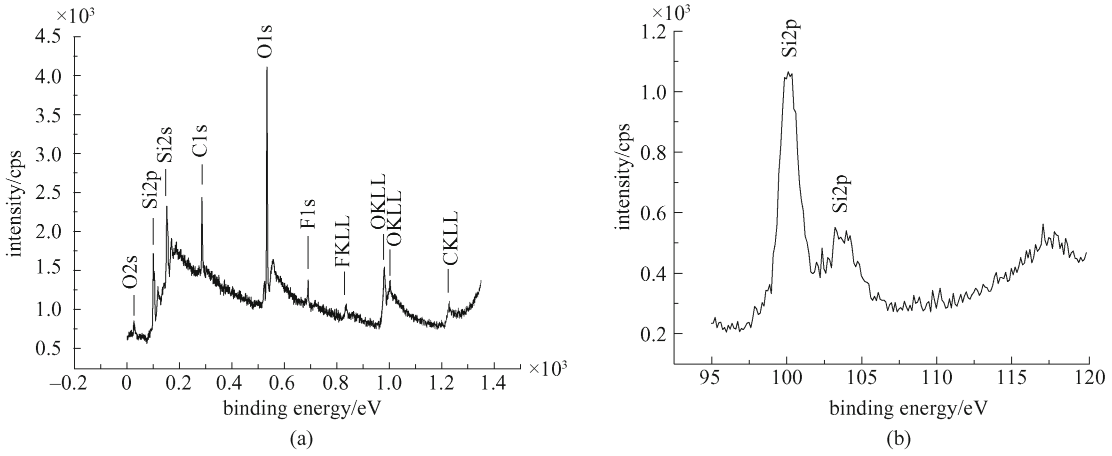

(a) (b)

Fig. 10 Element composition of machined surface detected by XPS. (a) General element composition; (b) composition of Si element

The gas diffusion in the process and heat distribution on the sample surface was first studied by the finite element analysis method. Then, the results were confirmed by corresponding experiments. It is demonstrated that the predicted temperature gradient is really formed in practical operation and the highest temperature on the wafer surface is just 90°C. The actual removal profile also accords well with the gas diffusion model, which also indicates a 32 mm^3/min removal rate on single crystal silicon wafers. By measuring the surface roughness before and after operations, a distinct contrast can be made showing obvious improvement of the surface state. The results also indicate an Ra 0.631 nm surface roughness which proves the capability of APPP to achieve the subnanometer scale polishing process. The XPS detection results provide references for further recipe improvement and process optimization.

Acknowledgements This work was supported by the National Natural Science Foundation of China (Grant Nos. 50535020, 50775055), the Defense Advanced Research Foundation (No. 9140A180202-06HT0132), the Natural Science Foundation of Heilongjiang Province (No. E200622).

References

1. Gao H G, Cao J L, Zhu Y, et al. The development and application of ultra-smooth surfaces. Physics, 2000, 29(10): 610–614 (in Chinese)
2. Gao H G, Chen B, Cao J L. Fabricating technology for supersmooth surfaces. Optics and Precision Engineering, 1995, 3(4): 7–14 (in Chinese)
3. Li X S, Ge H Z. Machining technologies for ultra-smooth surfaces. Laser and Optoelectronics Progress, 1998, 35(11): 1–9 (in Chinese)
4. Carr J W. Atmospheric pressure plasma processing for damage-free optics and surfaces. Engineering Research Development and Technology, 1999, 3: 31–39
5. Mori Y, Yamamura K, Endo K,et al. Creations of perfect surfaces. Journal of Crystal Growth, 2005, 275(1–2): 39–50
6. Mori Y, Yamauchi K, Yamamura K, et al. Development of plasma chemical vaporization machining. Review of Scientific Instruments, 2000, 71(12): 4627–4632
7. Zhang J F, Wang B, Dong S. A new development of ultra-smooth surface machining technology. Optical Technique, 2007, 33(suppl): 150–154 (in Chinese)
8. Zhang J F, Wang B, Dong S. Process monitoring and analysis in the atmospheric pressure plasma polishing (APPP) method. In: Yang L, Chen Y L, Kley E B, et al, eds. Advanced Optical Manufacturing Technologies. Chengdu: SPIE, 2008, 67220O
9. Zhang J F, Wang B, Dong S. The design of an atmospheric pressure plasma torch used for polishing ultra-smooth surfaces. Key Engineering Materials, 2008, 346–366: 340–345
10. Ke Y K, Dong H R. Analytical Chemistry Manual (III): Spectral Analysis. 2nd ed. Beijing: Chemical Industry Press, 1998, 50 (in Chinese)
11. Ke Y K, Dong H R. Analytical Chemistry Manual (III): Spectral Analysis. 2nd ed. Beijing: Chemical Industry Press, 1998, 19 (in Chinese)
12. Fanara C, Shore P, Nicholl J R. A new reactive atom plasma technology (RART) for precision machining: the etching of ULE optical surfaces. In: Eli A E eds. Opto-mechanical Technologies for Astronomy. Joseph Antebi and Dietrich Lemke: SPIE, 2006, 62730A
13. Okada H, Inagaki K, Goto H, et al. First-principles molecular-dynamics calculations and STM observations of dissociative adsorption of Cl_2 and F_2 on Si(100) surface. Surface Science, 2002, 515(2–3): 287–295
14. Carter L E, Carter E A. F_2 reaction dynamics with defective Si(100): defect-insensitive surface chemistry. Surface Science, 1995, 323(1–2): 39–50
15. Shibahara M, Katsuki M. Molecular dynamics study of the effects of adsorbed molecules on reaction probability and energy transfer. Combustion and Flame, 2006, 144(1–2): 17–23